Article

Chinese Science Bulletin

Geography

June 2011 Vol.56 No.16: 1714–1720
doi: 10.1007/s11434-011-4418-y

Is the maximum carbon number of long-chain *n*-alkanes an indicator of grassland or forest? Evidence from surface soils and modern plants

RAO ZhiGuo[1,2], WU Yi[1,3], ZHU ZhaoYu[1*], JIA GuoDong[1] & HENDERSON Andrew[4]

[1] *Key Laboratory of Marginal Sea Geology, Guangzhou Institute of Geochemistry, Chinese Academy of Sciences, Guangzhou 510640, China;*
[2] *Key Laboratory of Western China's Environmental Systems (Ministry of Education), Lanzhou University, Lanzhou 730000, China;*
[3] *Graduate University of Chinese Academy of Sciences, Beijing 100049, China;*
[4] *School of Geographical & Earth Sciences, University of Glasgow, Glasgow G12 8QQ, UK*

Received November 10, 2010; accepted December 23, 2010

The molecular distribution of long-chain *n*-alkanes in 62 soil samples collected from diverse locations across eastern China was analyzed. The long-chain *n*-alkanes were mostly dominated by *n*-C_{29} or *n*-C_{31}, regardless of the overlying vegetation type at each site. The results were compared with those summarized from the literature, covering more than 100 soil samples within China and more than 300 genera of modern plants distributed worldwide. There were similar *n*-alkane distribution patterns for most genera, with no clear differences among grasses, shrubs, and trees. The evidence from analyses of surface soils and modern plants indicates that the relationship between the molecular distribution of long-chain *n*-alkanes of surface soils and source vegetation is highly complex, and is influenced by many factors. Further, it is suggested that source vegetation types should not be simply inferred from distribution patterns of long-chain *n*-alkanes in sediments.

surface soils, modern plants, long-chain *n*-alkanes, molecular distribution, vegetation type

Citation: Rao Z G, Wu Y, Zhu Z Y, et al. Is the maximum carbon number of long-chain *n*-alkanes an indicator of grassland or forest? Evidence from surface soils and modern plants. Chinese Sci Bull, 2011, 56: 1714–1720, doi: 10.1007/s11434-011-4418-y

The evolution of terrestrial landscapes over geological time and modern history, including alternations between grassland and forest, has been driven by changes in the global climate. Efforts to reconstruct the history of terrestrial vegetation have mostly relied on the use of pollen [1,2] and phytolith [3] assemblages. Recently, the characteristic profiles of *n*-alkanes extracted from loess [4–6] and red clay [7,8] sediments have been used to reconstruct changes in vegetation over geological timescales. In some studies, the maximum carbon number (MCN) of long-chain *n*-alkanes, i.e., the carbon number of the most abundant homolog, has been used to indicate vegetation type. More specifically, it was suggested that long-chain *n*-alkanes dominated by *n*-C_{27} or *n*-C_{29} indicate forest, while those dominated by *n*-C_{31} indicate grassland. Therefore, the ratio of *n*-C_{27} to *n*-C_{31} (or *n*-C_{27}+*n*-C_{29}/*n*-C_{31}+*n*-C_{33}) has been used to represent the input of woody versus herbaceous plants.

Leaf waxes of higher terrestrial plants contain abundant long-chain *n*-alkanes with significant odd-to-even carbon number preference [9,10]. There are demonstrable links between the molecular distribution of long-chain *n*-alkanes of modern plants and different seasons, study sites, plant age, and plant organs [9]. Thus, there should be a complex relationship between the molecular distribution of sedimentary long-chain *n*-alkanes from multiple source plants and the source vegetation.

Even all the long-chain *n*-alkanes produced by woody plants are dominated by *n*-C_{27} or *n*-C_{29}, while those of herbaceous plants are dominated by *n*-C_{31}, it is unclear whether the MCN of material from multiple plant sources can be

*Corresponding author (email: zhuzy@gig.ac.cm)

© The Author(s) 2011. This article is published with open access at Springerlink.com

used to reconstruct the source vegetation type. It is possible that long-chain *n*-alkanes mixed from sources dominated by *n*-C_{27} (woody plants) and *n*-C_{31} (herbaceous plants) could be dominated by the *n*-C_{29}, because it occurs at relatively high concentrations in both of the source plant types. For example, if a woody plant with a ratio of 10∶7∶3 for *n*-C_{27}, *n*-C_{29}, and *n*-C_{31} and a herbaceous plant with a ratio of 1∶7∶10 for *n*-C_{27}, *n*-C_{29}, and *n*-C_{31} contributed equally to a certain sediment, the *n*-alkanes extracted from that sediment would show a ratio of 11∶14∶13 for *n*-C_{27}, *n*-C_{29}, and *n*-C_{31}. This would erroneously indicate that *n*-C_{29} was the dominant homolog in the source vegetation. Therefore, the MCN may not be a robust indicator of vegetation type, and the relative abundance of *n*-C_{27} to *n*-C_{31} does not indicate equal inputs from woody and herbaceous vegetation. Moreover, the production of long-chain *n*-alkanes may differ between different plants, which further complicate reconstructions of past vegetation.

Currently, there is no evidence that long-chain *n*-alkanes from woody plants are dominated by *n*-C_{27} and *n*-C_{29}, or that those of herbaceous plants are dominated by *n*-C_{31}. Similarly, there is little work showing how the MCN and molecular distribution of sedimentary long-chain *n*-alkanes from higher plants can be used to reconstruct paleovegetation. In this paper, we explore the relationship between the distribution of long chain *n*-alkanes and their respective vegetation sources based on the results from 100 surface soil samples collected from diverse areas across China and more than 300 globally distributed genera of modern plants.

1 Material and methods

For this study, a total of 62 surface soil samples were collected from diverse areas across China, extending from Hainan Province in southern China to Heilongjiang Province in northeastern China, spanning latitudes of 18°N to 50°N (Figure 1; Table S1). Vegetation across the study area ranges from tropical rainforest in southern China to temperate coniferous-deciduous broad-leaved mixed forest in northeastern China. The prevailing climate is monsoonal with concurrent rainy and hot seasons, with mean annual precipitation ranging from 500–2500 mm and a mean annual temperature of 0–26°C. The monsoonal climate trends from south to north with a strong dependence on latitude.

Surface soil samples were collected from the top 2–4 cm of weathering crust of basalt or other visible bedrocks in the field, thus avoiding contamination from underground water and allochthonous organic matter. The vegetation at all sampling sites was natural, with little human disturbance. Two to three surface samples were collected from different physiographic locations of each sampling site. A small grassland located in Damaping (114.5°E, 40.9°N, Figure 1), was sampled more intensively (12 samples). All samples

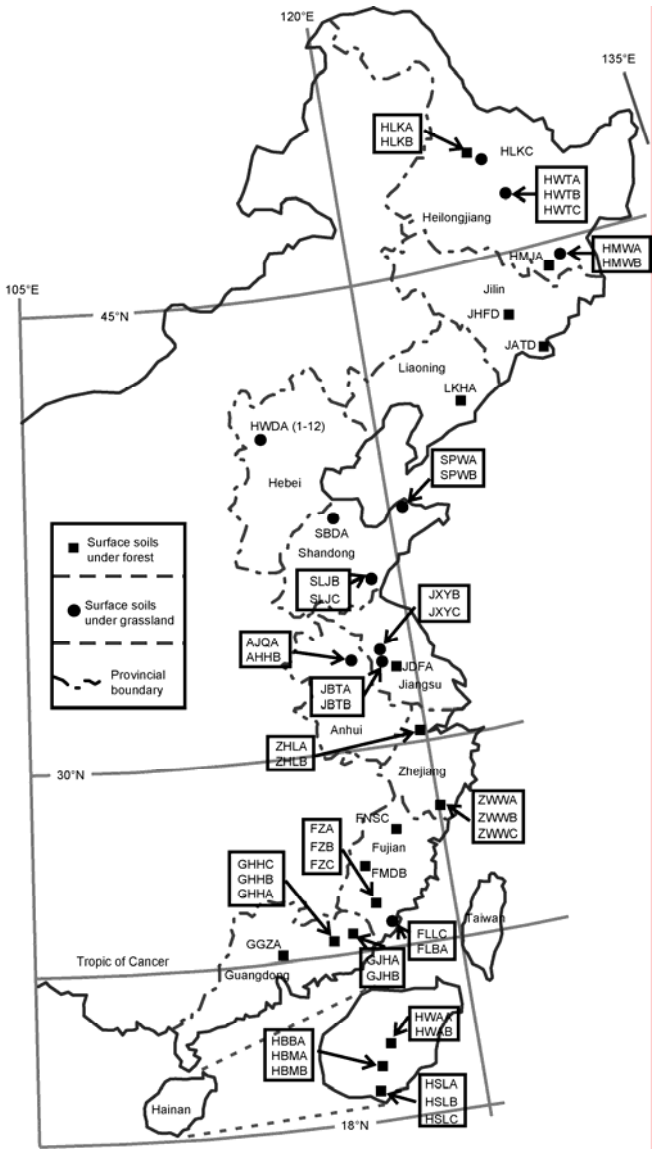

Figure 1 Map of study region and location of sampling sites.

were collected between September and November in 2005.

Rootlets and gravel were removed from the samples, and then they were ground and sieved through an 80-μm mesh sieve. After immersion in dichloromethane for ~2 h, approximately 10 g powdered soil was ultrasonically extracted for 10 min. This process was repeated three times and the combined solvents were then concentrated by rotary evaporation. The total lipid extract was separated using silica gel flash-column chromatography. The sample was eluted with hexane to obtain the saturated hydrocarbon fraction containing long-chain *n*-alkanes.

The long-chain *n*-alkanes were analyzed using an HP 6890 gas chromatograph equipped with an HP-5 MS silica capillary column (30 m × 0.32 mm × 0.25 μm). The oven temperature program was as follows: 80°C for 3 min, increasing to 200°C at a rate of 10°C/min, then increasing at

3°C/min to 290°C, and hold for 30 min. A reference material-Indiana STD (a set of *n*-alkanes consisting of 10 homologs; *n*-C_{12}, *n*-C_{14}, *n*-C_{16}, *n*-C_{18}, *n*-C_{20}, *n*-C_{22}, *n*-C_{25}, *n*-C_{28}, *n*-C_{30}, and *n*-C_{32}; Figure 2) was analyzed under exactly the same conditions. The carbon numbers of *n*-alkanes extracted from surface soil samples were determined by comparing their retention times with those of known alkanes in the reference material (Figure 2). The areas underneath *n*-alkane peaks were used to determine relative abundance.

2 Results and discussion

2.1 Long-chain *n*-alkanes extracted from surface soils under different vegetation types

The carbon numbers of *n*-alkanes extracted from most surface soil samples ranged from 14 to 35 with significant bimodal distribution (Figure 2). The short chain components without strong odd-to-even carbon number preference were dominated by either *n*-C_{17} or *n*-C_{19}. All samples showed relatively high concentrations of *n*-C_{23} to *n*-C_{34} alkanes with strong odd-to-even preference, with *n*-C_{27}, *n*-C_{29}, and *n*-C_{31} being the most dominant. The CPI (carbon preference index) of the long-chain *n*-alkanes extracted from all 62 surface soil samples ranged from 3 to 12.8 with an average value of 6.3. As reported in previous studies, *n*-C_{15} to *n*-C_{20} alkanes without significant odd-to-even preference and dominated by *n*-C_{17} or *n*-C_{19} alkanes are mainly derived from lower organisms [11], while terrestrial higher plants produce abundant long-chain *n*-alkanes with significant odd-to-even preference (such as *n*-C_{27}, *n*-C_{29}, and *n*-C_{31}) and with a CPI value exceeding 5 [9,12]. According to these classifications, the molecular distributions of *n*-alkanes extracted from our surface soil samples are characteristic of both higher plants and lower organisms, while the long-chain *n*-alkane components are derived from terrestrial higher plants.

We analyzed the MCN and relative abundance of the three main homologs (*n*-C_{27}, *n*-C_{29}, and *n*-C_{31}) of long-chain *n*-alkanes in each sample. Half of the samples (31) were collected from forested locations. The MCNs of *n*-alkanes in these samples were 27, 29, or 31, reflecting dominance of *n*-C_{27}, *n*-C_{29}, or *n*-C_{31} alkanes, respectively (Table S1; Figure 3). Of these 31 samples, 22 were dominated by *n*-C_{29}, 14 of which showed a relative abundance of *n*-C_{29}>*n*-C_{31}>*n*-C_{27}, and 8 of which showed a relative abundance of *n*-C_{29}>*n*-C_{27}>*n*-C_{31}. Of the remaining 9 samples, 5 were dominated by *n*-C_{27} with a relative abundance of *n*-C_{27}>*n*-C_{29}>*n*-C_{31}, and 4 were dominated by *n*-C_{31} with a relative abundance of *n*-C_{31}>*n*-C_{29}>*n*-C_{27}. Half of the samples (31) were collected from grassland. These had an MCN of 29 or 31, reflecting dominance of *n*-C_{29} or *n*-C_{31} alkanes, respectively. Of these 31 samples, 14 were dominated by *n*-C_{31} with a relative abundance of *n*-C_{31}>*n*-C_{29}>*n*-C_{27}. The other 17 samples were dominated by *n*-C_{29}; 13 samples showed a relative abundance of *n*-C_{29}>*n*-C_{31}>*n*-C_{27} and 4 samples showed a relative abundance of *n*-C_{29}>*n*-C_{27}>*n*-C_{31}.

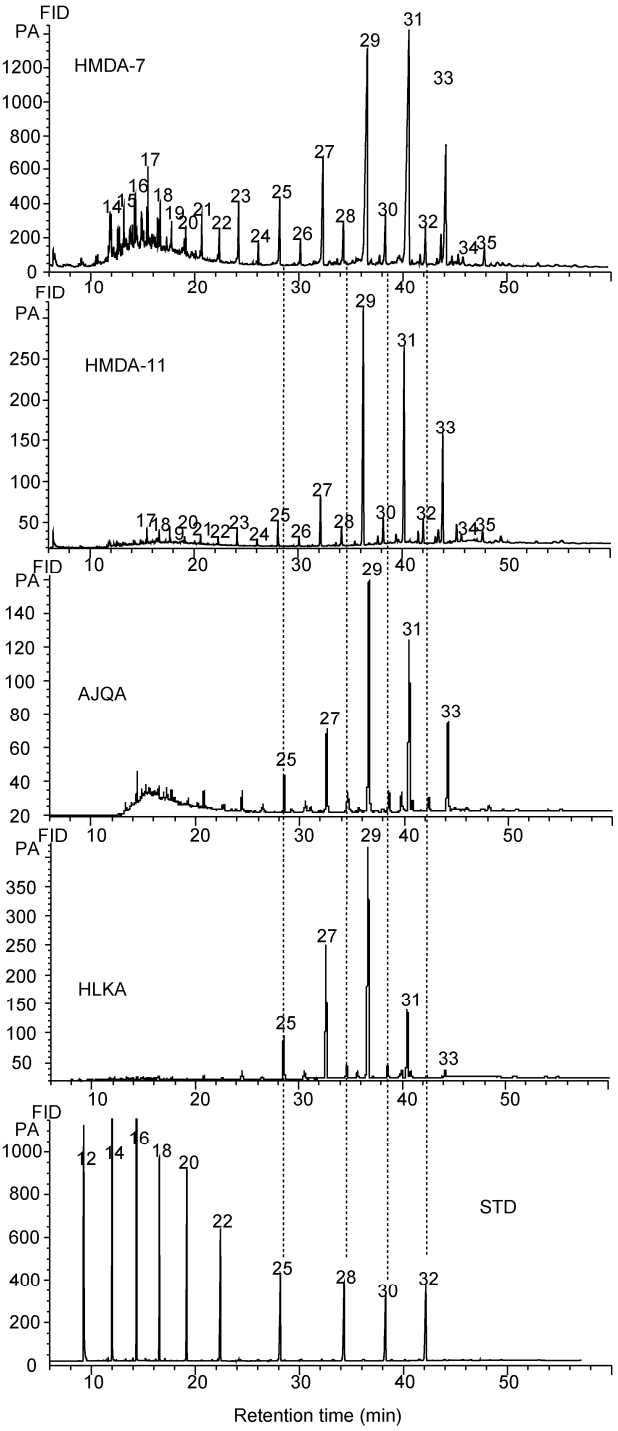

Figure 2 GC chromatogram of reference material and four typical surface soil samples (refer to Figure 1 and Table S1 for detailed information on soil samples).

The MCN and relative abundance of the three main homologs of long-chain *n*-alkanes varied among surface soil

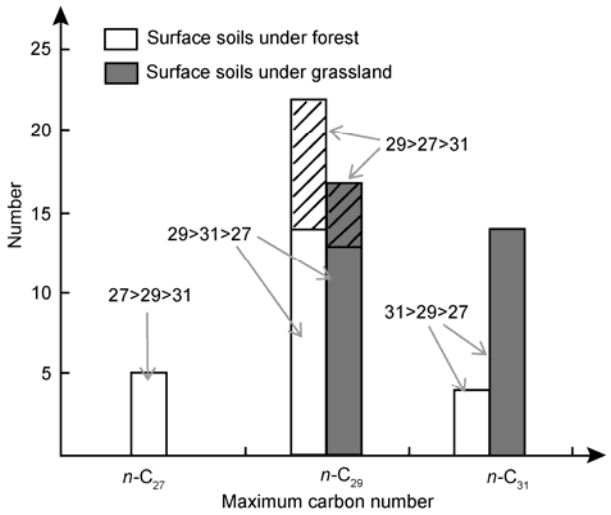

Figure 3 Maximum carbon number and relative abundance of three main homologs (n-C_{27}, n-C_{29}, and n-C_{31}) of long-chain n-alkanes extracted from 62 surface soil samples collected from across eastern China.

samples from the same location under the same vegetation. At the Damaping site (Figure 1), the bedrock is basalt and the top soil layer is too thin to support the growth of woody plants. Indeed, no woody plants were observed in the study area. Therefore, this location may have been influenced by grassland for a relatively long time. Of the 12 samples collected from this sampling site, 10 were dominated by n-C_{31} with a relative abundance of n-C_{31}>n-C_{29}>n-C_{27} (HMDA-7 in Figure 2). The remaining two samples were dominated by n-C_{29} with a relative abundance of n-C_{29}>n-C_{31}>n-C_{27} (HMDA-11 in Figure 2).

Most of the soil samples collected from across eastern China were dominated by n-C_{29} and n-C_{31} (only 5 out of 62 samples were dominated by n-C_{27}). This trend has also been reported in other studies. In a similar smaller study of 26 surface soil samples from China and Mongolia, most samples were dominated by n-C_{29} and n-C_{31} with n-C_{31} as the most frequent MCN, and only few samples were dominated by n-C_{27} [13]. In another study, n-alkanes of 10 surface soil samples from different climatic and vegetation zones were analyzed. Four from forested locations (three of which were plantation forests) were dominated by n-C_{29}, which were suggested to reflect a mixture of woody and herbaceous source plants, and 6 samples from grassy locations were dominated by n-C_{31} [14]. Long-chain n-alkanes extracted from surface soil in the Heshang Cave, Qingjiang, Hebei Province, were dominated by n-C_{31} [15]. Long-chain n-alkanes extracted from 9 surface soil samples collected from across the Loess Plateau were mainly dominated by n-C_{29} and n-C_{31}, while only few samples were dominated by n-C_{27} [16]. All of these surface soil samples were obtained from diverse locations with various overlying vegetation types and plant assemblages across a huge geographical region; however, the long-chain n-alkanes extracted from these samples were mainly and consistently dominated by n-C_{29} and n-C_{31}.

2.2 Long-chain *n*-alkanes extracted from different modern plants

We conducted a systematic evaluation of long-chain n-alkane distribution from 334 genera of modern plants reported in published studies [2,5,17–41] and unpublished data (Rao et al. personal unpublished data; Table S2). Most plants are dominated by n-C_{29} and n-C_{31}, even when they are divided into different groups such as trees, shrubs, and grasses (Table S2). Of the 207 modern grasses, 124 were dominated by n-C_{31} and 39 by n-C_{29}. Of the 101 modern trees, 35 genera showed an MCN reflecting n-C_{31} and 31 showed an MCN reflecting n-C_{29}. Of the 26 modern shrubs, 6 showed an MCN reflecting n-C_{31} and 15 showed an MCN reflecting n-C_{29} (Figure 4). Overall, 80% of grasses, 65% of trees, and 80% of shrubs were dominated by either n-C_{31} or n-C_{29}. Although this is a small sample size compared with the number of plant species worldwide, the data highlights that plants show common characteristics in the molecular distribution of long-chain n-alkanes.

2.3 Discussion

The relationship between the composition of long-chain n-alkanes in surface soils and the corresponding vegetation is complex, and there are many sources of uncertainty. It is possible that soils located under grasslands are affected by surrounding forests, and/or by deposition of atmospheric aerosols that act as a source of long-chain n-alkanes [42,43]. Considering the consistent odd-to-even preference and molecular distribution of long-chain n-alkanes from surface soils, it is likely that their variability results from overlying vegetation. For example, the n-alkane distribution in soils mainly dominated by n-C_{29} and n-C_{31} is similar to that identified in modern plants, regardless of the type of vegetation and plant.

Several studies on n-alkanes in soils have been carried out on red earth in southern China, including 12 Pleistocene samples from Changxing, Zhejiang Province [8], 52 Pleistocene samples from Xuancheng, Anhui Province [7] and

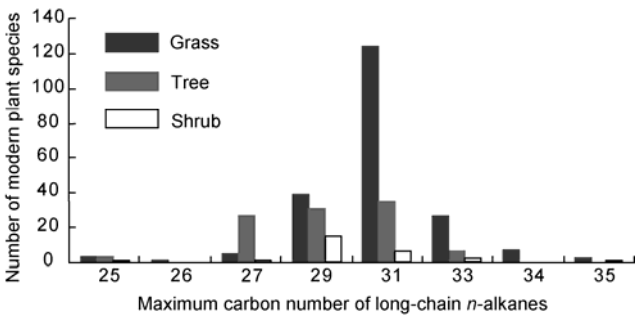

Figure 4 Maximum carbon number of long-chain n-alkanes extracted from modern plants, summarized from data in Table S2.

some Pleistocene samples from Xiushui, Jiangxi Province [44]. All of those samples were dominated by n-C_{29} or n-C_{31}. Analyses of samples from the Chinese Loess Plateau in northern China, including the Yuanbao profile in Linxia [45], the Dadiwan profile in Qin'an [5], the Caoxian profile [46], the Xifeng profile [47], and the Luochuan profile [4,6], showed a predominance of n-C_{31}, with only few samples dominated by n-C_{29}. Thus, in the red earth areas in southern China and loess areas in northern China, almost all samples were dominated by n-C_{29} and n-C_{31}, although it is unclear whether red earth or loess directly affects the n-alkane distribution in surface soils and modern plants in those areas. Together, these data indicate that there is a complex relationship between the molecular distribution of long-chain n-alkanes in surface soil and sediment derived from multiple plant sources and the type of source vegetation. There are several factors that control the molecular distribution of sedimentary n-alkanes, and therefore, affect their relationship with modern vegetation. These factors can be summarized as follows:

(1) Production of n-alkanes in plants: This can strongly influence the n-alkane profile, because a plant species that produces greater amounts of n-alkanes will bias the distribution of n-alkanes in sediments. Thus, the n-alkane profile of the sediment will not reflect the dominant vegetation. Differences in n-alkane production among plants in China have been reported [20]. In one study, the concentration of total n-alkanes from 93 gramineous plants ranged from 6.9 to 1860 μg/g with an average value of 164.1 μg/g [18]. Therefore, it is possible that the distribution of n-alkanes in sedimentary sequences reflects the plant source(s) with greatest n-alkane production rates, rather than those contributing the most biomass. Indeed, there is no evidence to suggest that the dominant plant shows the highest rate of n-alkanes production. On the contrary, there were no detectable n-alkanes in fresh pine needles of Lodgepole Pine (*Pinus contorta*), the dominant plant in a Canadian coniferous forest [19]. Likewise, the concentrations of n-alkanes extracted from some coniferous needles from Scandinavian regions were too low to permit isotopic measurement [17].

(2) Mixing effect of different sources: as mentioned above, a mixture of long-chain n-alkanes dominated by n-C_{27} and n-C_{31} may produce a signal indicating dominance of n-C_{29}, as all of the vegetation sources may contain relatively high concentrations of n-C_{29}. This is one possible reason why n-C_{29} is frequently the dominant component in surface soils and sediments. A recent study highlights this, as the molecular distribution of terrestrial n-alkanes in lake sediments was not characteristic of the dominant vegetation around the lake [17]. In that study, the authors analyzed diverse vegetation types and surface lake sediments collected from a wide geographical range (northern Finland to southern Italy). Their results may reflect, at least partly, the mixing process of n-alkanes.

(3) Variation of long-chain n-alkanes from the same plant under different environmental conditions, and post-depositional alteration: Some studies have argued there is no significant variation in the MCN and the molecular distribution of long-chain n-alkanes during the decomposition process [16] or in different growth seasons [15]. However, there is a large body of evidence that variation and alterations do occur [17,19,35,38,39]. Results from Europe indicate that the molecular distributions of n-alkanes within the same species vary among different study sites, and the average chain length (ACL) of n-alkanes from deciduous tree leaves increases from northern to southern Europe [17]. Some studies have reported varied molecular distribution of n-alkanes from the same species across different study sites (Table S2). Together, these findings indicate that the molecular distribution of n-alkanes in modern plants varies significantly depending on the prevailing climatic and environmental conditions.

All of these factors result in a very complex relationship between the molecular distribution of sedimentary long-chain n-alkanes and their respective source vegetation. At present, it is uncertain whether it is valid to use molecular distributions of long-chain n-alkanes, and particularly the MCN of long-chain n-alkanes, as indicators of source vegetation.

3 Conclusions

In this study, analyses of long-chain n-alkanes in 62 surface soil samples highlighted that the molecular distribution of long-chain n-alkanes of surface soils is highly variable, even among different sites with the same type of vegetation (forest or grassland). However, there were similar molecular distributions of long-chain n-alkanes in surface soils under different vegetation types (forest and grassland). Of the 62 samples, most (57) were dominated by n-C_{29} or n-C_{31} (only 5 were dominated by n-C_{27}), regardless of the type of overlying vegetation. This is consistent with the findings of other surface soil studies [13–16]. More importantly, the patterns of n-alkane distribution in more than 100 surface soils are consistent with those reported for more than 300 modern plant species [2,5,17–41], because most modern plants, whether they are trees, grasses, or shrubs, are also dominated by n-C_{29} and n-C_{31}. These results confirm that long-chain n-alkanes extracted from soils or sediments are derived from terrestrial higher plants. However, they cannot accurately predict the source vegetation because of the complex relationship between the molecular distribution of sedimentary long-chain n-alkanes (including both surface soils and sediments) and the type of source vegetation. That is, there is no simple model of interpretation. Therefore, for a given and specific set of long-chain n-alkanes that are dominated by n-C_{29} or n-C_{31}, it is almost impossible to determine whether they are derived from herbaceous or woody plants, or whether they represent forest or grassland vegetation.

This work was supported by the National Natural Science Foundation of China (40901055), the Key Project of the Chinese Ministry of Education (109151), the Fund for Creative Research Groups (41021091), the Cross-discipline Innovative Study Fund for Youth Talent of Lanzhou University (LZUJC2007011) and the National Basic Research Program of China (2010CB950202 and 2010CB833405).

1 Sun X J, Song C Q, Wang F Y, et al. Vegetation history of the Loess Plateau of China during the last 100000 years based on pollen data. Quat Int, 1997, 37: 25–36
2 Schwark L, Zink K, Lechterbeck L. Reconstruction of postglacial to early Holocene vegetation history in terrestrial Central Europe via cuticular lipid biomarkers and pollen records from lake sediments. Geology, 2002, 30: 463–466
3 Lü H Y, Liu D S, Wu N Q, et al. Phytolith record of vegetation succession in the southern Loess Plateau since late Pleistocene (in Chinese). Quat Sci, 1999, 4: 336–349
4 Yang M S, Zhang H C, Lei G L, et al. Biomarkers in weakly developed paleosol (L1SS1) in the Luochuan loess section and reconstructed paleovegetation-environment during the interstade of the Last Glaciation (in Chinese). Quat Sci, 2006, 26: 976–984
5 Zhong Y X, Chen F H, An C B, et al. Holocene vegetation cover in Qin'an area of western Chinese Loess Plateau revealed by *n*-alkane. Chinese Sci Bull, 2007, 52: 1692–1698
6 Zhang H C, Yang M S, Zhang W X, et al. Molecular fossil and paleovegetation records of paleosol S_4 and adjacent loess layers in the Luochuan loess section, NW China. Sci China Earth Sci, 2008, 51: 321–330
7 Liang B, Xie S C, Gu Y S, et al. Distribution of *n*-alkanes as indicative of paleovegetation change in Pleistocene red earth in Xuancheng, Anhui (in Chinese). J Earth Sci, 2005, 30: 129–132
8 Wang Z Y, Yu J H, Gu Y S, et al. Molecular fossils as indicators for paleoenvironment from quaternary red earth in Changxing, Zhejiang (in Chinese). Mar Geol Quat Geol, 2002, 22: 97–102
9 Eglinton G, Hamilton R J. Leaf epicuticular waxes. Science, 1967, 156: 1322–1334
10 Freeman K H, Hayes J M, Trendel J M, et al. Evidence from carbon isotope measurements for diverse origins of sedimentary hydrocarbons. Nature, 1990, 343: 254–256
11 Cranwell P A. Lipid geochemistry of sediments from Upton Broad, a small productive lake. Org Geochem, 1984, 7: 25–37
12 Rieley G, Collier R J, Jones D M, et al. The biogeochemistry of Ellesmere Lake, U.K. I: Source correlation of leaf wax inputs to the sedimentary lipid record. Org Geochem, 1991, 17: 901–912
13 Wang Y L, Fang X M, Bai Y, et al. Distribution of lipids in modern soils from various regions with continuous climate (moisture-heat) change in China and their climate significance. Sci China Earth Sci, 2007, 50: 600–612
14 Wang Z Y, Liu Z H, Yi Y, et al. Features of lipids and their significance in modern soils from various climate-vegetation regions (in Chinese). Acta Pedol Sin, 2003, 40: 967–970
15 Cui J W, Huang J H, Pu Y, et al. Comparison of lipid compositions between plant leaves and overlying soil in Heshang Cave, Qingjiang, Hubei Province and its significance (in Chinese). Quat Sci, 2007, 28: 35–42
16 Zhong Y X, Xue Q, Chen F H. *n*-alkane distributions in modern vegetation and surface soil from western Loess Plateau (in Chinese). Quat Sci, 2009, 29: 767–773
17 Sachse D, Radke J, Gleixner G. δD values of individual *n*-alkanes from terrestrial plants along a climatic gradient—Implications for the sedimentary biomarker record. Org Geochem, 2006, 37: 469–483
18 Maffei M. Chemotaxonomic significance of leaf wax alkanes in the Gramineae. Biochem Syst Ecol, 1996, 24: 53–64
19 Otto A, Simpson M J. Degradation and preservation of vascular plant-derived biomarkers in grassland and forest soils from Western Canada. Biogeochemistry, 2005, 74: 377–409
20 Cui J W, Huang J H, Xie S C. Characteristics of seasonal variations of leaf *n*-alkanes and *n*-alkenes in modern higher plants in Qingjiang, Hubei Province, China. Chinese Sci Bull, 2008, 53: 2659–2664
21 Bi X H, Sheng G Y, Liu X H, et al. Molecular and carbon and hydrogen isotopic composition of *n*-alkanes in plant leaf waxes. Org Geochem, 2005, 36: 1405–1417
22 Chikaraishi Y, Naraoka H. Compound-specific δD-δ^{13}C analyses of *n*-alkanes extracted from terrestrial and aquatic plants. Phytochemistry, 2003, 63: 361–371
23 Chikaraishi Y, Naraoka H, Poulson S R. Carbon and hydrogen isotopic fractionation during lipid biosynthesis in a higher plant (*Cryptomeria japonica*). Phytochemistry, 2004, 65: 323–330
24 Conte M H, Weber J C, Carlson P J, et al. Molecular and carbon isotopic composition of leaf wax in vegetation and aerosols in a northern prairie ecosystem. Oecologia, 2003, 135: 67–77
25 Gormann R, Schreiber L, Kolodziej H. Cuticular wax profiles of leaves of some traditionally used African Bignoniaceae. Z Naturforsch, 2004, 59: 631–635
26 Huang Y, Eglinton G, Ineson P, et al. Absence of carbon isotope fractionation of individual *n*-alkanes in a 23-year field decomposition experiment with *Calluna valgaris*. Org Geochem, 1997, 26: 497–501
27 Jansen B, Nierop K, Hageman J, et al. The straight-chain lipid biomarker composition of plant species responsible for the dominant biomass production along two altitudinal transects in the Ecuadorian Andes. Org Geochem, 2006, 37: 1514–1536
28 Kawamura K, Ishimura Y, Yamazaki K. Four years' observations of terrestrial lipid class compounds in marine aerosols from the western North Pacific. Glob Biogeochem Cycle, 2003, 17: 1003, doi: 10.1029/2001GB001810
29 Krull E, Sachse D, Mügler I, et al. Compound-specific δ^{13}C and δ^{2}H analyses of plant and soil organic matter: A preliminary assessment of the effects of vegetation change on ecosystem hydrology. Soil Biol Biochem, 2006, 38: 3211–3221
30 Li B C, Dong Y L, Li C, et al. Distribution and compound specific carbon isotope of individual long chain alkanes from leaves of *Kandelia Candel* and *Ficus Microcarpa* and their photosynthesis (in Chinese). J Trop Oceanol, 2003, 22: 62–69
31 Liu W G, Huang Y S. Compound-specific D/H ratios and molecular distributions of higher plant leaf waxes as novel paleoenvironmental indicators in the Chinese Loess Plateau. Org Geochem, 2005, 36: 851–860
32 Lockheart M J, Van Bergen P F, Evershed R P. Variations in the stable carbon isotope compositions of individual lipids from the leaves of modern angiosperms: Implications for the study of higher land plant-derived sedimentary organic matter. Org Geochem, 1997, 26: 137–153
33 Lockheart M J, Van Bergen P F, Evershed R P. Chemotaxonomic classification of fossil leaves from the Miocene Clarkia lake deposit, Idaho, USA based on *n*-alkyl lipid distributions and principal component analyses. Org Geochem, 2000, 31: 1223–1246
34 Marseille F, Disnar J, Guillet B, et al. *n*-Alkanes and free fatty acids in humus and A1 horizons of soils under beech, spruce and grass in the Massif-Central (Mont-Lozère), France. Eur J Soil Sci, 1999, 50: 433–441
35 Mügler I, Sachse D, Werner M, et al. Effect of lake evaporation on δD values of lacustrine *n*-alkanes: A comparison of Nam Co (Tibetan Plateau) and Holzmaar (Germany). Org Geochem, 2008, 39: 711–729
36 Nichols J E, Booth R K, Jackson S T, et al. Paleohydrologic reconstruction based on *n*-alkane distributions in ombrotrophic peat. Org Geochem, 2006, 37: 1505–1513
37 Nott C J, Xie S C, Avsejs L A, et al. *n*-alkane distributions in ombrotrophic mires as indicators of vegetation change related to climatic variation. Org Geochem, 2000, 31: 231–235
38 Rommerskirchen F, Plader A, Eglinton G, et al. Chemotaxonomic significance of distribution and stable carbon isotopic composition of long-chain alkanes and alkan-1-ols in C_4 grass waxes. Org Geochem, 2006, 37: 1303–1332
39 Sessions A L. Seasonal changes in D/H fractionation accompanying lipid biosynthesis in *Spartina alterniflora*. Geochim Cosmochim Acta,

2006, 70: 2153–2162
40 Wiesenberg G L B, Schmidt M W I, Schwark L. Plant and soil lipid modifications under elevated atmospheric CO_2 conditions: I. Lipid distribution patterns. Org Geochem, 2008, 39: 91–102
41 Xie S C, Nott C J, Avsejs L A, et al. Molecular and isotopic stratigraphy in ombrotrophic mire for paleoclimate reconstruction. Geochim Cosmochim Acta, 2004, 68: 2849–2862
42 Guo F Q, Zhang C J, Zhang Y, et al. Distribution of *n*-alkane and environmental significance about the Lanzhou atmospheric dust (in Chinese). Environ Sci Technol, 2009, 32: 9–11
43 Xie M J, Wang G H, Hu S Y, et al. Aliphatic alkanes and polycyclic aromatic hydrocarbons in atmospheric PM_{10} aerosols from Baoji, China: Implications for coal burning. Atmos Res, 2009, 93: 840–848
44 Xie S C, Yi Y, Liu Y Y, et al. The Pleistocene vermicular red earth in South China signaling the global climatic change: The molecular fossil record. Sci China Earth Sci, 2003, 46: 1114–1120
45 Wang Z Y, Xie S C, Chen F H. *n*-Alkane distribution as indicator for paleo-vegetation: An example from Yuanbao S_1 paleosol in Linxia, Gansu Province (in Chinese). Quat Sci, 2004, 24: 231–235
46 Zhong Y X. Environmental change in western Chinese Loess Plateau since the Last Glacial: Organic geochemical records in Loess (in Chinese). Dissertation for the Doctoral Degree. Lanzhou: Lanzhou University, 2008. 60–90
47 Liu W G, Huang Y S, An Z S, et al. Summer monsoon intensity controls C_4/C_3 plants abundanceduring the last 35 ka in the Chinese Loess Plateau: Carbon isotope evidence from bulk organic matter and individual leaf waxes. Palaeogeogr Palaeoclimatol Palaeoecol, 2005, 220: 243–254

Open Access This article is distributed under the terms of the Creative Commons Attribution License which permits any use, distribution, and reproduction in any medium, provided the original author(s) and source are credited.

Supporting Information

Table S1 Detailed information on 62 surface soil samples collected from across eastern China, and composition of long-chain *n*-alkanes

Table S2 Maximum carbon number of long-chain *n*-alkanes extracted from modern plants and references

The supporting information is available online at csb.scichina.com and www.springerlink.com. The supporting materials are published as submitted, without typesetting or editing. The responsibility for scientific accuracy and content remains entirely with the authors.

Sample code[1)]	Bedrock type	Vegetation type	Longitude (°E)	Latitude (°N)	Altitude (m)	temperature (°C)	precipitation (mm)	maximum carbon number	C_{27}/C_{31}	CPI[2)] (23～34)	ACL[3)] (25～33)	Relative abundance
HLKA	basalt	forest	125.79	49.22	371	-0.1	480.8	29	1.82	12.75	28.51	*n*-C_{29}> *n*-C_{27}> *n*-C_{31}
HLKB	basalt	forest	125.79	49.22	444	-0.1	480.8	27	4.12	12.34	27.86	*n*-C_{27}> *n*-C_{29}> *n*-C_{31}
HLKC	basalt	grassland	125.79	49.23	310	-0.1	480.8	29	0.84	9.16	28.90	*n*-C_{29}> *n*-C_{31}> *n*-C_{27}
HWTA	basalt	grassland	126.00	48.61	276	0.4	521.5	29	0.99	8.49	28.80	*n*-C_{29}> *n*-C_{31}> *n*-C_{27}
HWTB	basalt	grassland	126.00	48.61	275	0.4	521.5	29	1.17	8.47	28.68	*n*-C_{29}> *n*-C_{27}> *n*-C_{31}
HWTC	basalt	grassland	126.00	48.61	273	0.4	521.5	29	1.42	6.02	28.28	*n*-C_{29}> *n*-C_{27}> *n*-C_{31}
HMWA	basalt	grassland	129.58	44.48	357	3.8	531.0	29	1.99	4.12	28.17	*n*-C_{29}> *n*-C_{27}> *n*-C_{31}
HMWB	basalt	grassland	129.58	44.48	336	3.8	531.0	29	1.06	8.62	28.88	*n*-C_{29}> *n*-C_{27}> *n*-C_{31}
HMJA	basalt	forest	128.53	44.19	868	3.8	531.0	29	3.12	7.38	28.09	*n*-C_{29}> *n*-C_{27}> *n*-C_{31}
JATD	basalt	forest	128.06	42.04	1960	2.2	657.2	29	1.18	9.54	28.61	*n*-C_{29}> *n*-C_{27}> *n*-C_{31}
JHFD	basalt	forest	126.44	42.38	746	2.9	737.9	29	1.73	8.34	28.50	*n*-C_{29}> *n*-C_{27}> *n*-C_{31}
LKHA	basalt	forest	124.75	40.73	518	6.7	1093.9	29	1.65	5.93	28.58	*n*-C_{29}> *n*-C_{27}> *n*-C_{31}
SBDA	basalt	grassland	117.68	38.01	34	12.3	584.6	29	0.74	7.05	29.42	*n*-C_{29}> *n*-C_{31}> *n*-C_{27}
SPWA	basalt	grassland	120.72	37.78	129	12.6	687.6	33	0.46	4.91	30.21	*n*-C_{31}> *n*-C_{29}> *n*-C_{27}
SPWB	basalt	grassland	120.72	37.78	118	12.6	687.6	31	0.32	6.39	29.96	*n*-C_{31}> *n*-C_{29}> *n*-C_{27}
SLJB	unknown	grassland	118.84	35.22	194	13.3	849.0	29	0.25	8.25	29.93	*n*-C_{29}> *n*-C_{31}> *n*-C_{27}
SLJC	unknown	grassland	118.84	35.22	145	13.3	849.0	29	0.44	6.17	29.36	*n*-C_{29}> *n*-C_{31}> *n*-C_{27}
JXYB	basalt	grassland	118.34	32.90	138	14.6	994.0	29	0.63	5.08	29.29	*n*-C_{29}> *n*-C_{31}> *n*-C_{27}
JXYC	basalt	grassland	118.35	32.89	128	14.6	994.0	29	0.74	8.73	29.14	*n*-C_{29}> *n*-C_{31}> *n*-C_{27}
AJQA	basalt	grassland	118.26	32.81	130	15.2	904.0	29	0.45	8.04	29.70	*n*-C_{29}> *n*-C_{31}> *n*-C_{27}
AHHB	basalt	grassland	118.00	32.63	144	15.2	904.0	29	0.55	4.19	29.58	*n*-C_{29}> *n*-C_{31}> *n*-C_{27}
JDFA	basalt	forest	118.98	32.31	102	15.3	1034.1	29	0.86	5.40	29.12	*n*-C_{29}> *n*-C_{31}> *n*-C_{27}

JBTA	basalt	grassland	118.95	32.41	78	15.3	1034.1	29	0.50	3.39	29.39	*n*-C_{29}> *n*-C_{31}> *n*-C_{27}
JBTB	basalt	grassland	118.96	32.41	73	15.3	1034.1	29	0.68	4.77	29.34	*n*-C_{29}> *n*-C_{31}> *n*-C_{27}
ZHLA	unknown	forest	120.01	30.35	57	16.2	1374.7	29	0.46	4.96	29.50	*n*-C_{29}> *n*-C_{31}> *n*-C_{27}
ZHLB	unknown	forest	120.01	30.35	29	16.2	1374.7	29	0.80	4.10	29.19	*n*-C_{29}> *n*-C_{31}> *n*-C_{27}
ZWWA	unknown	forest	120.64	27.96	175	17.9	1675.0	29	1.15	4.22	28.94	*n*-C_{29}> *n*-C_{27}> *n*-C_{31}
ZWWB	unknown	forest	120.64	27.96	167	17.9	1675.0	29	0.65	4.44	29.34	*n*-C_{29}> *n*-C_{31}> *n*-C_{27}
ZWWC	unknown	forest	120.64	27.96	151	17.9	1675.0	29	0.66	4.65	29.21	*n*-C_{29}> *n*-C_{31}> *n*-C_{27}
FNSC	unknown	forest	118.77	27.53	56	18.1	1696.5	31	0.19	4.27	29.93	*n*-C_{31}> *n*-C_{29}> *n*-C_{27}
FMDB	basalt	forest	117.12	26.41	635	19.2	1567.6	29	0.88	4.65	29.25	*n*-C_{29}> *n*-C_{31}> *n*-C_{27}
FZA	unknown	forest	117.41	25.30	225	19.9	1724.7	27	1.29	4.08	29.13	*n*-C_{27}> *n*-C_{29}> *n*-C_{31}
FZB	unknown	forest	117.41	25.30	232	19.9	1724.7	29	0.63	3.61	29.61	*n*-C_{29}> *n*-C_{31}> *n*-C_{27}
FZC	unknown	forest	117.41	25.30	208	19.9	1724.7	29	1.69	4.28	28.65	*n*-C_{29}> *n*-C_{27}> *n*-C_{31}
FLLC	basalt	grassland	118.14	24.27	63	20.1	1318.6	31	0.25	6.10	30.18	*n*-C_{31}> *n*-C_{29}> *n*-C_{27}
FLBA	basalt	grassland	118.04	24.22	46	20.1	1318.6	31	0.23	5.67	30.04	*n*-C_{31}> *n*-C_{29}> *n*-C_{27}
GJHA	unknown	forest	116.37	23.58	83	21.2	1531.2	27	4.89	4.64	27.90	*n*-C_{27}> *n*-C_{29}> *n*-C_{31}
GJHB	unknown	forest	116.37	23.58	75	21.2	1531.2	27	5.55	5.32	27.91	*n*-C_{27}> *n*-C_{29}> *n*-C_{31}
GHHA	unknown	forest	114.61	23.16	30	21.8	1716.6	31	0.52	3.04	29.64	*n*-C_{31}> *n*-C_{29}> *n*-C_{27}
GHHB	unknown	forest	114.61	23.16	47	21.8	1716.6	31	0.49	3.41	29.88	*n*-C_{31}> *n*-C_{29}> *n*-C_{27}
GHHC	unknown	forest	114.61	23.16	23	21.8	1716.6	31	0.74	3.95	29.33	*n*-C_{31}> *n*-C_{29}> *n*-C_{27}
GGZA	granite	forest	113.50	23.11	28	21.8	1681.9	27	3.15	5.77	28.37	*n*-C_{27}> *n*-C_{29}> *n*-C_{31}
HSLA	granite	forest	109.55	18.33	39	25.6	1266.7	29	0.56	5.23	28.89	*n*-C_{29}> *n*-C_{31}> *n*-C_{27}
HSLB	granite	forest	109.54	18.32	36	25.6	1266.7	29	0.71	4.87	29.07	*n*-C_{29}> *n*-C_{31}> *n*-C_{27}
HSLC	granite	forest	109.54	18.31	14	25.6	1266.7	29	0.60	4.38	29.17	*n*-C_{29}> *n*-C_{31}> *n*-C_{27}
HBBA	granite	forest	109.67	18.41	165	25.6	1266.7	29	0.78	4.37	29.17	*n*-C_{29}> *n*-C_{31}> *n*-C_{27}
HBMA	granite	forest	109.57	18.61	439	25.6	1266.7	29	0.68	4.90	29.19	*n*-C_{29}> *n*-C_{31}> *n*-C_{27}
HBMB	granite	forest	109.56	18.61	500	25.6	1266.7	29	0.78	4.51	29.10	*n*-C_{29}> *n*-C_{31}> *n*-C_{27}

HWAA	granite	forest	109.51	18.83	794	22.5	2458.5	29	1.67	5.32	28.40	*n*-C_{29}> *n*-C_{27}> *n*-C_{31}
HWAB	granite	forest	109.51	18.83	794	22.5	2458.5	29	0.44	5.33	29.54	*n*-C_{29}> *n*-C_{31}> *n*-C_{27}
HZDA-1	basalt	grassland	114.51	40.98	1750	8.3	398.5	31	0.17	9.43	30.21	*n*-C_{31}> *n*-C_{29}> *n*-C_{27}
HZDA-2	basalt	grassland	114.51	40.98	1740	8.3	398.5	31	0.25	8.01	29.99	*n*-C_{31}> *n*-C_{29}> *n*-C_{27}
HZDA-3	basalt	grassland	114.51	40.98	1730	8.3	398.5	31	0.17	8.52	30.27	*n*-C_{31}> *n*-C_{29}> *n*-C_{27}
HZDA-4	basalt	grassland	114.51	40.98	1720	8.3	398.5	31	0.18	8.72	30.28	*n*-C_{31}> *n*-C_{29}> *n*-C_{27}
HZDA-5	basalt	grassland	114.51	40.98	1715	8.3	398.5	31	0.21	5.50	30.15	*n*-C_{31}> *n*-C_{29}> *n*-C_{27}
HZDA-6	basalt	grassland	114.51	40.98	1700	8.3	398.5	31	0.26	6.40	29.99	*n*-C_{31}> *n*-C_{29}> *n*-C_{27}
HZDA-7	basalt	grassland	114.51	40.98	1680	8.3	398.5	31	0.25	7.90	29.95	*n*-C_{31}> *n*-C_{29}> *n*-C_{27}
HZDA-8	basalt	grassland	114.51	40.98	1670	8.3	398.5	31	0.24	7.36	30.03	*n*-C_{31}> *n*-C_{29}> *n*-C_{27}
HZDA-9	basalt	grassland	114.51	40.98	1650	8.3	398.5	31	0.14	10.10	30.16	*n*-C_{31}> *n*-C_{29}> *n*-C_{27}
HZDA-10	basalt	grassland	114.51	40.98	1640	8.3	398.5	31	0.23	8.47	30.11	*n*-C_{31}> *n*-C_{29}> *n*-C_{27}
HZDA-11	basalt	grassland	114.51	40.98	1590	8.3	398.5	29	0.22	7.40	30.08	*n*-C_{29}> *n*-C_{31}> *n*-C_{27}
HZDA-12	basalt	grassland	114.51	40.98	1490	8.3	398.5	29	0.31	6.27	29.91	*n*-C_{29}> *n*-C_{31}> *n*-C_{27}

1) Sample code as the same as Figure 1
2) CPI- carbon preference index
3) ACL-average chain length

Name or code of Plant	Type of Plant	Maximum carbon number	Location	Reference
Alternanthera bettzickiana	grass	31	Guangzhou, China	[21]
Alternanthera dentata	grass	29	Guangzhou, China	[21]
Alternanthera versicolor	grass	31	Guangzhou, China	[21]
Amaranthus paniculatus	grass	31	Guangzhou, China	[21]
Amaranthus tricolor	grass	31	Guangzhou, China	[21]
Araucaria cunninghamii	tree	31	Guangzhou, China	[21]
Bothriochloa ischaemum	grass	31	Guangzhou, China	[21]
Caryota mitis	tree	31	Guangzhou, China	[21]
Cinnamomum burmanni	tree	31	Guangzhou, China	[21]
Codiaeum variegatum	shrub	33	Guangzhou, China	[21]
Euphorbia pulcherrima	shrub	29	Guangzhou, China	[21]
Ficus altissima	tree	31	Guangzhou, China	[21]
Ficus microcarpa	tree	31	Guangzhou, China	[21]
Holmskioldia sanguinea	shrub	35	Guangzhou, China	[21]
Imperata cylindrica	grass	31	Guangzhou, China	[21]
Kigelia africana (am.)	tree	31	Guangzhou, China	[21]
Osmanthus fragrans	tree	31	Guangzhou, China	[21]
Saccharum sinense	grass	27	Guangzhou, China	[21]
Swietenia mahagoni	tree	31	Guangzhou, China	[21]
Syzygium cumini	tree	31	Guangzhou, China	[21]
Zea mays	grass	29	Guangzhou, China	[21]
Zoysia japonica	grass	33	Guangzhou, China	[21]
Acer argutum	tree	31	Gunma, Japan	[22]
Acer argutum	tree	31	Gunma, Japan	[22]
Acer carpinifolium	tree	31	Gunma, Japan	[22]
Acer carpinifolium	tree	31	Gunma, Japan	[22]
Acer palmatum	tree	31	Gunma, Japan	[22]
Albizia julibrissin	tree	29	Ogasawara, Japan	[22]
Artemisia princeps	grass	31	Gunma, Japan	[22]
Benthamidia japonica	shrub	29	Gunma, Japan	[22]
Benthamidia japonica	shrub	29	Gunma, Japan	[22]
Camellia sasanqua	shrub	29	Tokyo, Japan	[22]
Chamaecyparis obtusa	tree	33	Tokyo, Japan	[22]
Cryptomeria japonica	tree	33	Gunma, Japan	[22]
Cryptomeria japonica	tree	33	Gunma, Japan	[22]
Manihot utilissima	shrub	31	Thailand	[22]
Miscanthus sinensis	grass	31	Tokyo, Japan	[22]
Miscanthus sinensis	grass	29	Gunma, Japan	[22]
Phrogmites communis	grass	29	Gunma, Japan	[22]
Pinus thunbergii	tree	29	Tokyo, Japan	[22]
Plantago asiatica	grass	31	Gunma, Japan	[22]

Prunus jamasakura	shrub	29	Gunma, Japan	[22]
Quercus acutissima	tree	29	Tokyo, Japan	[22]
Quercus dentata	tree	29	Gunma, Japan	[22]
Quercus mongolica	tree	29	Gunma, Japan	[22]
Saccharum officinarum	grass	31	Okinawa, Japan	[22]
Saccharum officinarum	grass	33	Thailand	[22]
Sorghum bicolor	grass	31	Thailand	[22]
Taraxacum officinale	grass	29	Gunma, Japan	[22]
Zea mays	grass	33	Tokyo, Japan	[22]
Zoysia japonica	grass	33	Tokyo, Japan	[22]
Acer argutum	tree	31	Gunma, Japan	[22]
Acer carpinifolium	tree	31	Gunma, Japan	[22]
Cryptomeria japonica	tree	33	Japan (in both spring and autumn)	[23]
Agropyron smithii	grass	31	Alberta, Canada	[24]
Bouteloua gracilis	grass	31	Alberta, Canada	[24]
Brassica napus	grass	29	crops, Alberta, Canada	[24]
Hordeum vulgare	Shrub	33	crops, Alberta, Canada	[24]
Medicago sativa	grass	31	crops, Alberta, Canada	[24]
Stipa viridula	grass	31	Alberta, Canada	[24]
Tragopogon dubius	grass	31	Alberta, Canada	[24]
Triticum aestivum	grass	29	crops, Alberta, Canada	[24]
Kigelia africana	tree	31	Botanical Garden of Berlin, Germany	[25]
Markhamia acuminata	tree	33	Botanical Garden of Berlin, Germany	[25]
Newbouldia laevis	tree	31	Royal Botanical Garden, Belgium	[25]
Spathodea campanulata	tree	33	Botanical Garden of Berlin, Germany	[25]
Culluna vulgaris	shrub	31	Bog Hill, UK	[26]
Calamagrostis effusa	grass	31	Ecuadorian Andes	[27]
Rhynchospora ruiziana	grass	31	Ecuadorian Andes	[27]
Espeletia pycnophylla	shrub	29	Ecuadorian Andes	[27]
Oreobolus goeppingeri	grass	29	Ecuadorian Andes	[27]
Gaiadendron punctatum	shrub	29	Ecuadorian Andes	[27]
Blechnum schomburgkii	tree	27	Ecuadorian Andes	[27]
Miconia tinifolia	tree	29	Ecuadorian Andes	[27]
Weinmannia cochensis	tree	29	Ecuadorian Andes	[27]
Neurolepis aristata	grass	29	Ecuadorian Andes	[27]
Gynoxys buxifolia	tree	29	Ecuadorian Andes	[27]
Clusia flaviflora	tree	29	Ecuadorian Andes	[27]
Tillandsia sp.2	tree	29	Ecuadorian Andes	[27]
Hedyosmum cumbalense	shrub	25	Ecuadorian Andes	[27]
Vallea stipularis	tree	27	Ecuadorian Andes	[27]
Macleania rupestris	shrub	29	Ecuadorian Andes	[27]

Juncus balticus ssp. Andicola	grass	31	Ecuadorian Andes	[27]
Plantago australis	grass	33	Ecuadorian Andes	[27]
Lachemilla andina	grass	33	Ecuadorian Andes	[27]
Oreobolus obtusangulus	grass	31	Ecuadorian Andes	[27]
Birch	tree	29	Hokkaido,Japan	[28]
Theaceae	tree	29	Chichi-Jima Island, Japan	[28]
unknown species	tree	31	Bidadari Island, Indonesia	[28]
Acacia cambagei	tree	29	Queensland, Australia	[29]
Astrebla pectinata	grass	31	Queensland, Australia	[29]
Atalaya hemiglauca	tree	31	Queensland, Australia	[29]
Iseilema spp.	grass	31	Queensland, Australia	[29]
Ficus microcarpa	tree	27	Haikou, Hainan, China	[30]
Kadelia candel	tree	27	Shenzhen,Guangdong, China	[30]
Kadelia candel	tree	27	Xinzhu,Hainan, China	[30]
Kadelia candel	tree	25	Yangjiang,Guangdong, China	[30]
Artemisia scoparia	shrub	29	Chinese Loess Plateau	[31]
Heteropappus Less	grass	31	Chinese Loess Plateau	[31]
Stipa krylovii	grass	31	Chinese Loess Plateau	[31]
Cleistogenes Keng	grass	29	Chinese Loess Plateau	[31]
Haloxylon ammodendron	shrub	27	Chinese Loess Plateau	[31]
Pennisetum flaccidum	grass	31	Chinese Loess Plateau	[31]
Salsola collina	shrub	29	Chinese Loess Plateau	[31]
Stipa bungeana	grass	31	Chinese Loess Plateau	[31]
Fagus sylvatica	tree	27	Gloucestershire, UK	[32]
Fagus grandifolia	tree	29	unknown	[33]
Metasequoia glyptostroboides	tree	25	Gloucestershire, UK	[33]
Quercus marilandica	tree	29	unknown	[33]
Achnaterum calamagrostis	grass	31	Turin, Italy	[18]
Agropyron pungens	grass	34	Turin, Italy	[18]
Agropyron repens	grass	34	Turin, Italy	[18]
Agrostis alba	grass	29	Turin, Italy	[18]
Agrostis albaf	grass	33	Turin, Italy	[18]
Agrostis alpina	grass	31	Turin, Italy	[18]
Agrostis stolonifera	grass	34	Turin, Italy	[18]
Alopecurus gerardi	grass	25	Turin, Italy	[18]
Ampelodesmos tenax	grass	31	Turin, Italy	[18]
Anthoxantum odoratum	grass	31	Turin, Italy	[18]
Arrhenaterum elatius	grass	29	Turin, Italy	[18]
Arundo donax	grass	29	Turin, Italy	[18]
Avena fatua	grass	29	Turin, Italy	[18]
Avena parlatorei	grass	31	Turin, Italy	[18]
Avena versicolor	grass	33	Turin, Italy	[18]

Brachypodium pinnatum	grass	31	Turin, Italy	[18]
Brachypodium stylvaticum	grass	31	Turin, Italy	[18]
Briza media	grass	31	Turin, Italy	[18]
Bromus catharticus	grass	31	Turin, Italy	[18]
Bromus erectus	grass	31	Turin, Italy	[18]
Bromus hordeaceus	grass	31	Turin, Italy	[18]
Bromus sterilis	grass	31	Turin, Italy	[18]
Calamagrostis arundinacea	grass	31	Turin, Italy	[18]
Calamagrostis epigejon	grass	31	Turin, Italy	[18]
Calamagrostis villosa	grass	29	Turin, Italy	[18]
Coix lacryma-Jobi	grass	31	Turin, Italy	[18]
Cortaderia selloana	grass	31	Turin, Italy	[18]
Cymbopogon citratus	grass	31	Turin, Italy	[18]
Cynodon dactylon	grass	33	Turin, Italy	[18]
Cynosurus echinatus	grass	29	Turin, Italy	[18]
Dactylis glomerata	grass	31	Turin, Italy	[18]
Dactyloctenium aegyptium	grass	31	Turin, Italy	[18]
Digitaria sanguinalis	grass	35	Turin, Italy	[18]
Echinochloa colonum	grass	33	Turin, Italy	[18]
Echinochloa crus-galli	grass	27	Turin, Italy	[18]
Echinochloa phyllopogon	grass	27	Turin, Italy	[18]
Eleusine indica	grass	31	Turin, Italy	[18]
Elymus glganteus	grass	34	Turin, Italy	[18]
Elymus pungens	grass	34	Turin, Italy	[18]
Elymus virginicus	grass	29	Turin, Italy	[18]
Festuca arundinacea	grass	31	Turin, Italy	[18]
Festuca cinerea	grass	31	Turin, Italy	[18]
Festuca ovina	grass	31	Turin, Italy	[18]
Festuca ovina var duriuscola	grass	31	Turin, Italy	[18]
Festuca pratensis	grass	31	Turin, Italy	[18]
Festuca rubra	grass	31	Turin, Italy	[18]
Festuca spadicea	grass	29	Turin, Italy	[18]
Festuca varia	grass	29	Turin, Italy	[18]
Festuca violacea	grass	29	Turin, Italy	[18]
Holcus lanatus	grass	27	Turin, Italy	[18]
Holcus mollis	grass	25	Turin, Italy	[18]
Hordeum murinum	grass	34	Turin, Italy	[18]
Koeleria valesiaca	grass	31	Turin, Italy	[18]
L.multiflorum	grass	31	Turin, Italy	[18]
Lagurus ovatus	grass	26	Turin, Italy	[18]
Lolium italicum	grass	31	Turin, Italy	[18]
Melica ciliata	grass	31	Turin, Italy	[18]
Melica picta	grass	31	Turin, Italy	[18]

Miscanthus sinensis	grass	31	Turin, Italy	[18]
Nardus stricta	grass	29	Turin, Italy	[18]
Oryza sativa	grass	31	Turin, Italy	[18]
Pennisetum americanum	grass	31	Turin, Italy	[18]
Phalaris arundinacea	grass	29	Turin, Italy	[18]
Phalaris canariensis	grass	31	Turin, Italy	[18]
Phleum alpinum	grass	29	Turin, Italy	[18]
Phleum bertolonii	grass	31	Turin, Italy	[18]
Phleum pratense	grass	31	Turin, Italy	[18]
Phragmites australis	grass	29	Turin, Italy	[18]
Phyllostachys bambusoides	grass	29	Turin, Italy	[18]
Poa annus	grass	25	Turin, Italy	[18]
Poa festucaeformis	grass	31	Turin, Italy	[18]
Poa nemorlis	grass	31	Turin, Italy	[18]
Poa pratensis	grass	31	Western Italian Alps.	[18]
Poa pratensis	grass	31	Turin, Italy	[18]
Poa vivipara	grass	31	Turin, Italy	[18]
Saccharum officinarum	grass	31	Turin, Italy	[18]
Saccharum spontaeum	grass	29	Turin, Italy	[18]
Secale cereale	grass	34	Turin, Italy	[18]
Secale montanum	grass	31	Turin, Italy	[18]
Setaria glauca	grass	33	Turin, Italy	[18]
Setaria italica	grass	31	Turin, Italy	[18]
Sorgum halepense	grass	31	Turin, Italy	[18]
Sorgum vulgare	grass	31	Turin, Italy	[18]
Stipa calamagrostis	grass	31	Turin, Italy	[18]
Stipa calamagrostis	grass	31	Western Italian Alps.	[18]
Stipa capillata	grass	31	Turin, Italy	[18]
Stipa tenacissima	grass	31	Turin, Italy	[18]
Stipa thessala	grass	31	Turin, Italy	[18]
Trisetum flavescens	grass	31	Turin, Italy	[18]
Triticum durum	grass	29	Turin, Italy	[18]
Triticum vulgare	grass	29	Turin, Italy	[18]
Vetiveria zizanioides	grass	31	Turin, Italy	[18]
Zea mays	grass	31	Turin, Italy	[18]
Fagus sylvatica	tree	27	Massif-Central, France	[34]
Picea abies	tree	27	Massif-Central, France	[34]
Kobresia schoenoides	grass	29	Tibet, China	[35]
Kobresia schoenoides	grass	29	Tibet, China	[35]
Kobresia schoenoides	grass	31	Tibet, China	[35]
Kobresia schoenoides	grass	31	Tibet, China	[35]
Morina sp.	grass	31	Tibet, China	[35]
Morina sp.	grass	31	Tibet, China	[35]
Oxytropis sp.	grass	29	Tibet, China	[35]

Stipa	grass	31	Tibet, China	[35]
Stipa sp.	grass	31	Tibet, China	[35]
Chamydaphne calyculata	shrub	29	NY, UAS	[36]
Kalmia polifolia	shrub	29	NY, UAS	[36]
Rhododenderon groenlandicum	shrub	31	NY, UAS	[36]
Andromeda polifolia	shrub	31	Cumbria, UK	[37]
Calluna vulgaris	tree	31	Cumbria, UK	[37]
Empetrum nigrum	shrub	31	Cumbria, UK	[37]
Erica tetralix	tree	31	Cumbria, UK	[37]
Eriophorum angustifolium	grass	31	Cumbria, UK	[37]
Eriophorum vaginatum	grass	31	Cumbria, UK	[37]
Rhynchospora alba	grass	31	Cumbria, UK	[37]
Trichophorum cespitosum	grass	31	Cumbria, UK	[37]
Vaccinium oxycoccus	shrub	29	Cumbria, UK	[37]
Agropyron smithii	grass	31	green grass, Albert, Canada	[19]
Agropyron smithii	grass	29	decomposing grass, Albert, Canada	[19]
Agropyron smithii	grass	29	green grass, Albert, Canada	[19]
Populus tremula	tree	25	Alberta, Canada	[19]
Pinus contorta	tree	29	leaf litter, Albert, Canada	[19]
Cinnamonum campora	tree	31	Changsha, Hunan, China	personal unpublished data
Corylus heterophylla	tree	29	Changsha, Hunan, China	personal unpublished data
Liquidambar formosana	tree	31	Changsha, Hunan, China	personal unpublished data
Oryza Sativa	grass	29	Changsha, Hunan, China	personal unpublished data
Paulownia tomentosa	tree	31	Changsha, Hunan, China	personal unpublished data
Zea mays	grass	31	Changsha, Hunan, China	personal unpublished data
Aristida adscensionis	grass	31	Namibia	[38]
Aristida barbicollis	grass	31	Zimbabwe	[38]
Aristida congesta	grass	31	Namibia	[38]
Aristida graciliflora	grass	31	Zimbabwe	[38]
Aristida meridionalis	grass	31	Zimbabwe	[38]
Aristida meridionalis	grass	31	Namibia	[38]
Bothriochloa insculpta	grass	31	Zimbabwe	[38]
Brachiaria erucitormis	grass	33	Zimbabwe	[38]
Brachiaria sp.	grass	33	Tanzania	[38]
Bromus sp.	grass	31	Australia	[38]
Chloris gayana	grass	33	Zimbabwe	[38]
Chloris virgata	grass	33	Zimbabwe	[38]
Chloris virgata	grass	31	Namibia	[38]
Digitaria milanjiana	grass	33	Zimbabwe	[38]
Enneapogon cenchroides	grass	31	Zimbabwe	[38]
Enneapogon cenchroides	grass	31	Namibia	[38]
Enneapogon sp.	grass	33	Namibia	[38]

Eragrostis nindensis	grass	31	Namibia	[38]
Eragrostis superba	grass	27	Zimbabwe	[38]
Eragrostis tremula	grass	31	Sudan	[38]
Eragrostis violacea de winter	grass	31	Zimbabwe	[38]
Eragrostis viscosa	grass	29	Zimbabwe	[38]
Festuca orthophylla	grass	29	Peru	[38]
Festuca orthophylla	grass	29	Peru	[38]
Hyparrhenia filipendula	grass	33	Zimbabwe	[38]
Loudetia simplex	grass	31	Zimbabwe	[38]
Panicum arbusculum	grass	33	Namibia	[38]
Panicum maximum	grass	31	Zimbabwe	[38]
Panicum maximum	grass	31	Namibia	[38]
Panicum sp.	grass	33	Namibia	[38]
Schmidtia kalahariensis	grass	33	Namibia	[38]
Sporobolus ioclados	grass	33	Zimbabwe	[38]
Sporobolus pyramidalis	grass	33	Zimbabwe	[38]
Sporobolus sp.	grass	33	Tanzania	[38]
Stipagrostis ciliata	grass	31	Namibia	[38]
Stipagrostis hirtigluma	grass	31	Namibia	[38]
Stipagrostis uniplumis	grass	31	Namibia	[38]
Themeda triandra	grass	31	Zimbabwe	[38]
Aluns incana	tree	29	MAS (ITA)	[17]
Betula pendula	tree	27	NAI (FIN)	[17]
Betula pendula	tree	27	SOD007 (FIN)	[17]
Betula pendula	tree	27	SOD004 (FIN)	[17]
Betula pendula	tree	27	HYY (FIN)	[17]
Betula pendula	tree	27	SYR (FIN)	[17]
Betula pendula	tree	31	LAM (FIN)	[17]
Betula pendula	tree	31	HZM (GER)	[17]
Betula pubescens	tree	27	FIN002 (FIN)	[17]
Betula pubescens	tree	27	KEI	[17]
Betula pubescens	tree	27	SOD003 (FIN)	[17]
Carpinus betulus	tree	31	MEZ (ITA)	[17]
Fagus sylvatica	tree	27	SOD003 (FIN)	[17]
Fagus sylvatica	tree	27	HZM (GER)	[17]
Fagus sylvatica	tree	27	LGM (ITA)	[17]
Myrtus	tree	31	SYR (FIN)	[17]
Quercus cerris	tree	29	MAS (ITA)	[17]
Quercus petraea	tree	29	MEZ (ITA)	[17]
Quercus robur	tree	29	ITA001 (ITA)	[17]
Quercus variabilis	tree	31	MAS (ITA)	[17]
Artemisia vulgaris	grass	31	SW, Germany	[2]
Artemisin absinthum	grass	31	SW, Germany	[2]

Betula nana, alpine	tree	27	SW, Germany	[2]
Betula nana, arctic	tree	27	SW, Germany	[2]
Betula pendula (alba)	tree	31	SW, Germany	[2]
Betula pubescens	tree	27	SW, Germany	[2]
Juniperus comm.	tree	31	SW, Germany	[2]
Pinus cerbra	tree	31	SW, Germany	[2]
Pinus mugo	tree	29	SW, Germany	[2]
Pinus nigra	tree	31	SW, Germany	[2]
Pinus sylvestris	tree	29	SW, Germany	[2]
Spartina alterniflora	grass	29	Massachusetts, USA (dead leaves)	[39]
Spartina alterniflora	grass	31	Massachusetts, USA (new leaves)	[39]
Lolium perenne	grass	31	Switzerland	[40]
Trifolium repens	grass	29	Switzerland	[40]
Eriophorum angustifolium	grass	31	Cumbria, England	[41]
Eriophorum vaginatum	grass	31	Cumbria, England	[41]
Trichophorum cespitosum	grass	31	Cumbria, England	[41]
Larix spp.	tree	29	Chinese Loess Plateau	[5]
Pinus tabulaeformis	tree	29	Chinese Loess Plateau	[5]
XL-BH	tree	27	Chinese Loess Plateau	[16]
XL-QQ	tree	29	Chinese Loess Plateau	[16]
XL-LDL	tree	27	Chinese Loess Plateau	[16]
XL-SY	tree	27	Chinese Loess Plateau	[16]
SFG-HQ	shrub	29	Chinese Loess Plateau	[16]
SFG-HH	tree	27	Chinese Loess Plateau	[16]
SFG-QY	tree	29	Chinese Loess Plateau	[16]
LPS-LYS	tree	29	Chinese Loess Plateau	[16]
LPS-YS	tree	29	Chinese Loess Plateau	[16]
LD-QQ	tree	29	Chinese Loess Plateau	[16]
XL-JJR	shrub	29	Chinese Loess Plateau	[16]
XL-WSLMFJ	grass	31	Chinese Loess Plateau	[16]
XL-TC	grass	31	Chinese Loess Plateau	[16]
XL-MYWLC	grass	33	Chinese Loess Plateau	[16]
SFG_TC	grass	33	Chinese Loess Plateau	[16]
ZW-1	tree	31	Qingjiang, Hubei	[20]
ZW-3	grass	31	Qingjiang, Hubei	[20]
ZW-4	grass	35	Qingjiang, Hubei	[20]
ZW-6	tree	29	Qingjiang, Hubei	[20]
ZW-10	shrub	31	Qingjiang, Hubei	[20]